AD-A148 661 ELECTROCHEMICAL FEATURES OF THE FERRIC SULFATE LEACHING OF CUFES2/C AGGREGATES(U) UTAH UNIV SALT LAKE CITY DEPT OF CHEMISTRY R Y WAN ET AL. 28 NOV 84 TR-36 1/1

UNCLASSIFIED N00014-83-K-0470 F/G 7/2 NL

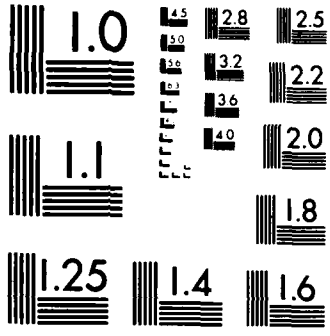

(12)

OFFICE OF NAVAL RESEARCH

Contract N00014-83-K-0470

Task No. NR 359-718

TECHNICAL REPORT NO. 36

Electrochemical Features of the Ferric Sulfate Leaching of $CuFeS_2$/C Aggregates

By

R. Y. Wan
J. D. Miller
J. Foley
Stanley Pons

Prepared for Publication in

Proc. Electrochem. Soc.

University of Utah
Department of Chemistry
Salt Lake City, Utah 84112

November 28, 1984

SECURITY CLASSIFICATION OF THIS PAGE (When Data Entered)

REPORT DOCUMENTATION PAGE		READ INSTRUCTIONS BEFORE COMPLETING FORM
1. REPORT NUMBER: 36	2. GOVT ACCESSION NO.: AD-A148 664	3. RECIPIENT'S CATALOG NUMBER:
4. TITLE (and Subtitle): Electrochemical Features of the Ferric Sulfate Leaching of $CuFeS_2$/C Aggregates		5. TYPE OF REPORT & PERIOD COVERED: Technical Report # 36
		6. PERFORMING ORG. REPORT NUMBER:
7. AUTHOR(s): R. Y. Wan; J. D. Miller; J. Foley; Stanley Pons		8. CONTRACT OR GRANT NUMBER(s): N00014-83-K-0470
9. PERFORMING ORGANIZATION NAME AND ADDRESS: University of Utah, Department of Chemistry, Salt Lake City, UT 84112		10. PROGRAM ELEMENT, PROJECT, TASK AREA & WORK UNIT NUMBERS: Task No. NR 359-718
11. CONTROLLING OFFICE NAME AND ADDRESS: Office of Naval Research, Chemistry Program - Chemistry Code 472, Arlington, Virginia 22217		12. REPORT DATE: November 28, 1984
		13. NUMBER OF PAGES: 26
14. MONITORING AGENCY NAME & ADDRESS (if different from Controlling Office)		15. SECURITY CLASS. (of this report): Unclassified
		15a. DECLASSIFICATION/DOWNGRADING SCHEDULE

16. DISTRIBUTION STATEMENT (of this Report)

This document has been approved for public release and sale; its distribution unlimited.

17. DISTRIBUTION STATEMENT (of the abstract entered in Block 20, if different from Report)

18. SUPPLEMENTARY NOTES

19. KEY WORDS (Continue on reverse side if necessary and identify by block number)

Chalcopyrites, Electrochemical etching

20. ABSTRACT (Continue on reverse side if necessary and identify by block number)

DD FORM 1 JAN 73 1473 EDITION OF 1 NOV 65 IS OBSOLETE

S/N 0102-LF-014-6601

Unclassified

SECURITY CLASSIFICATION OF THIS PAGE (When Data Entered)

Symposium Proceedings

Electrochemistry

ELECTROCHEMICAL FEATURES OF THE FERRIC SULFATE LEACHING OF $CuFeS_2$/C AGGREGATES

R. Y. Wan and J. D. Miller
J. Foley and S. Pons

Subject Index

page

ELECTROCHEMICAL FEATURES OF THE FERRIC SULFATE LEACHING OF $CuFeS_2$/C AGGREGATES

R. Y. Wan and J. D. Miller
Department of Metallurgy and Metallurgical Engineering

J. Foley and S. Pons
Department of Chemistry
University of Utah
Salt Lake City, Utah 84112

Abstract

The rate of chalcopyrite dissolution by ferric sulfate solution can be enhanced by the presence of conductive carbon particles. The addition of carbon has been found to increase the leaching rate of chalcopyrite by as much as a factor of four. The importance of carbon in the enhanced leaching of chalcopyrite has been discussed in previous publications. The same rate increase has been found to prevail for the initial reaction kinetics. To further evaluate the effect of carbon during the initial stage of reaction, the results from initial rate experiments are discussed in conjunction with polarization and spectroelectrochemical measurements.

The initial rate of the ferric sulfate leaching of $CuFeS_2$/C aggregates was found to be one-half order with respect to ferric concentration and inversely proportional to the initial particle diameter, with an apparent activation energy of 38.1 kJ/mole (9.1 kcal/mole). These initial rate characteristics are similar to those found for ferric sulfate leaching of chalcopyrite without carbon and suggest that in both cases the initial reaction rate is controlled by an electrochemical surface reaction. However, the initial rate is three times faster in the presence of carbon.

Electrochemical measurements further support these results. The corrosion current for the anodic reaction of $CuFeS_2$/C aggregate electrodes was found to be about five times greater than that for chalcopyrite electrodes without carbon addition. Satisfactory agreement exists between electrochemical measurements and the initial leaching rate. It is evident from the polarization curves that the galvanic coupling between carbon and chalcopyrite eliminates to some extent the passivating effect that has been observed by many investigators. These findings suggest that in the absence

of carbon the anodic and cathodic half-cell reactions do not experience the same potential because of the resistance of a passivating film. Finally, in-situ Fourier Transform Infrared spectroelectrochemical measurements have been made in an attempt to identify the surface reaction product during the initial stages of reaction.

INTRODUCTION

The acid ferric sulfate leaching of chalcopyrite has been studied extensively because of its significance in dump leaching practice and its potential for the hydrometallurgical processing of copper sulfide concentrates. However, the reaction kinetics are extremely slow and seem to be significantly influenced by the nature of the reaction product.

Ferric Sulfate Leaching Studies

Many researchers have attempted to explain the leaching behavior of chalcopyrite, but there is not complete agreement in the interpretation of the reaction kinetics. The ferric sulfate leaching reaction for chalcopyrite follows the equation

$$CuFeS_2 + 4Fe^{3+} = Cu^{2+} + 5Fe^{2+} + 2S^0 \qquad (1)$$

One of the most significant features of the reaction is the formation of a dense, tenacious sulfur layer. Some investigators believe that transport through this layer limits the reaction rate and explains the slow leaching rate of chalcopyrite. The very slow leaching kinetics of chalcopyrite in ferric sulfate solution has been established by many researchers (1-6). The significance of the elemental sulfur product layer in the leaching reaction can be appreciated from the experimental results shown in Figure 1. In these experiments the reaction was interrupted at 40% conversion and the sulfur removed by distillation under N_2 atmosphere below 500°C. When the leaching reaction was started again, after the sulfur product had been removed, the original initial reaction kinetics were obtained. The results in Figure 1 give further evidence that the protective sulfur reaction product forms a diffusion barrier and the dissolution rate becomes limited by transport through this insulating layer. This hypothesis is substantiated by other results which show that ferric sulfate leaching of chalcopyrite has an inverse second-order dependence on chalcopyrite particle size, a high activation energy, and an independence on stirring speed. These rate data have been successfully described using Wagner's theory of oxidation, which relates the electrical conductivity of elemental sulfur to the rate of reaction. Analysis of the ferric sulfate leaching system in this context suggests that the rate-limiting process is as depicted schematically in Figure 2.

If the reaction kinetics for ferric sulfate leaching of chalcopyrite are limited by electron transport in the elemental sulfur reaction product layer, modification of this reaction product layer to increase its conductivity should increase the rate of reaction.

It is expected that the electrical conductivity of an insulator phase (such as sulfur) may be altered by the addition of dispersed

conductors (7). Recently, Simkovich et al. (8) found that small additions of carbon black to elemental sulfur increased the electrical conductivity of the system by about 8 to 12 orders of magnitude. Assuming that carbon particles can be dispersed in the sulfur product layer and act in a similar manner, the dissolution rate of chalcopyrite in ferric sulfate solution would be expected to increase. In fact such an effect has been established and these results are summarized below.

Ferric Sulfate Leaching of $CuFeS_2$/C Aggregates

The extremely slow reaction kinetics of ferric sulfate leaching of chalcopyrite can be enhanced by the formation of $CuFeS_2$/C aggregates with particulate carbon (9). The ferric sulfate leaching of chalcopyrite from these aggregates has been found to increase by 400-600% (after 10 hours' leaching), depending upon the electrical conductivity of carbon and the carbon particle size, as shown in Figure 3. The attached carbon particles accelerate the chalcopyrite leaching rate, which may be explained in part by the improved transport of electrons through the sulfur reaction-product layer. The increase in the copper dissolution rate with respect to carbon type correlates with an increase in the electrical conductivity of the corresponding carbon/sulfur composites presented in Table 1. Also, the enhanced reaction rate is dependent upon the particle size and probably upon the number of carbon particles in contact with a chalcopyrite surface. The importance of compaction between carbon and chalcopyrite particles has been established by the experimental results shown in Figure 4. Although the leaching rate of the mixture of chalcopyrite and carbon particles (without pressing) is enhanced, it certainly is not as high as the compressed $CuFeS_2$/C pellets. It is interesting to note that the increased leaching rate is achieved at lower agitation speeds, as shown in Figure 4, presumably an indication that the aggregate integrity must be preserved. Also, it has been found that aggregates of chalcopyrite compacted with non-conductive particles such as talc, silica, or alumina do not leach at an enhanced rate. These results support the position that the conductive carbon particles change the conductivity of the reaction product layer and such a phenomenon accounts for the increase in leaching rate.

In addition to improved conductivity, the sulfur product layer has been found to have a more botryoidal, less protective character. As shown in Figures 5 and 6, the morphology of the elemental sulfur formed during the leaching of $CuFeS_2$/C aggregates ($CuFeS_2$/Monarch 800 = 25/1) differs significantly from the dense, tenacious sulfur which forms on the chalcopyrite surface in the absence of carbon.

Partially reacted samples of $CuFeS_2$/C aggregates were characterized by x-ray diffraction (XRD). Figure 7 indicates that the chalcopyrite peak decreases as the leaching reaction proceeds and the appearance of the elemental sulfur can be distinguished. From the data

shown in Figure 7, after 13 hours and 58% reaction, the elemental sulfur peak becomes quite evident at 2θ angles of 23.1, 25.8, and 27.8 degrees, and the $CuFeS_2$ peak has decreased considerably. In the absence of carbon, the elemental sulfur could not be detected by XRD. These results are similar to the results of previous investigators (1) who have had difficulty in identifying the elemental sulfur product by XRD and have described the sulfur as being amorphous. It seems that the presence of carbon promotes the growth of crystalline sulfur, and in fact it has been found that liquid sulfur (120°C) wets a carbon surface completely (5). The carbon particles would appear to be ideal sites for sulfur nucleation and growth.

Electrochemical Behavior of Chalcopyrite Electrodes

In addition to these leaching studies, considerable effort has been directed toward the electrochemical behavior of chalcopyrite electrodes in acid sulfate solution. Of course, this research, by design, has been limited to initial reaction behavior and does not necessarily describe rate control phenomena for a leaching reaction as it goes to completion.

Biegler and Swift (10) studied the anodic behavior of chalcopyrite in 1 M H_2SO_4 and 1 M HCl at room temperature by linear sweep voltametry and potentiostatic electrolysis. For example, they found in one case that the anodic reaction involved 6.7 ±0.3 F per mole of chalcopyrite. From this data, it was calculated that 86% of the sulfide sulfur was oxidized to the elemental form. Chalcopyrite dissolution occurred at localized sites, the number of which depended strongly on potential. The anodic dissolution of chalcopyrite in general was found to be a non-uniform process giving rise to pits and crevices on the electrode surface. At potentials about 0.76-0.86 volt vs. SCE, the sulfur formed was insoluble in carbon disulfide and was suggested to be an amorphous plastic form of sulfur. After standing over a period of days, the sulfur transformed to the rhombic form. No intermediate solid products were detected at the electrode surface. It was suggested that the physical properties of plastic sulfur may allow it to form the dense tenacious layer found in leaching experiments (1).

The results from other electrochemical studies at low temperatures indicate that the rate-limiting step for the anodic reaction is a surface reaction or diffusion through intermediate passive sulfide layers. Jones (11) carried out potentiostatic experiments in which he observed a decrease in current with time at low constant potentials. Other investigators (10,12) have presented similar decay curves. The continued current decay indicates that a progressively thickening passive film is formed. But the passive nature of the film was found to diminish as the potential was increased.

Warren et al. (13) studied the passive and transpassive anodic behavior of chalcopyrite in acid solutions at low temperature. Based on current and mass balance measurements, two intermediate phases, S_1 and S_2, appeared to form in the sequence

$$CuFeS_2 \rightarrow S_1 \rightarrow S_2 \quad (2)$$

In the first step of the reaction, ferrous ions are released much more rapidly than cupric ions, forming an intermediate structure according to the reaction

$$CuFeS_2 \rightarrow Cu_{1-x}Fe_{1-y}S_{2-z} + xCu^{2+} + yFe^{2+} + zS^o + 2ze^- \quad (3)$$

where $y > x$ initially. The compound or defect structure, $Cu_{1-x}Fe_{1-z}S_{2-z}$, was suggested to be an intermediate phase which, mixed with sulfur, forms an electron-conducting passive layer on the mineral surface. This sulfide film is referred to as S_1. Parker et al. (14) also refers to the intermediate product as a polysulfide having semiconducting properties. It was suggested that the first intermediate product S_1 decomposes to form a second intermediate S_2, releasing equal quantities of copper and iron, according to the following reaction:

$$Cu_{1-x}Fe_{1-y}S_{2-z} \rightarrow (2-z)CuS_{(n-s)} + (1-y)Cu^{2+} + (1-y)Fe^{2+} + 2(1-y)e^- \quad (4)$$

The $CuS_{(n-s)}$ represents a second, nonstoichiometric, intermediate phase S_2 which then decomposes to elemental sulfur at low potentials:

$$CuS_{(n-s)} \rightarrow Cu^{2+} + S^o + 2e^- \quad (5)$$

The growth of the passivation layer results in a rapid decay of current at low voltage. Similarly, Hillrichs et al. (15) concluded that in the transpassive potential range, the surface is mostly free of sulfur and the current density is mainly controlled by a thin passive layer.

Parker et al. (16) studied the electrochemical behavior of the oxidation leaching of chalcopyrite at elevated temperature (70-90°C) within the 0.2-0.6 volt (vs. SCE) region. They suggested that a semiconductor surface film, thought to be a metal-deficient polysulfide, forms on the chalcopyrite surface during anodic polarization. The metal-deficient polysulfide is thermally unstable and slows transport

of ions and slows electron transfer to oxidants. They concluded that this film accounts for the electrochemical and kinetic aspects of chalcopyrite leaching and that product sulfur is of little kinetic consequence in the leaching of chalcopyrite. Previously cited evidence would not support this conclusion. Importantly, it should be recognized that these electrochemical studies and the aforementioned conclusions must be limited, strictly speaking, to initial reaction behavior, and results from electrochemical studies do not necessarily account for leaching reaction kinetics when the reaction goes to completion.

To summarize, the overall leaching behavior of chalcopyrite is not necessarily explained by electrochemical measurements. Nevertheless, electrochemical measurements could explain the initial reaction kinetics, and in this regard such measurements are useful. Research efforts have been made to explain the increase in the initial rates of ferric sulfate leaching by the addition of conductive carbon particles to the system. In order to further evaluate the initial reaction kinetics, polarization curves for massive and particulate chalcopyrite electrodes in the presence and absence of carbon were determined. Finally, in-situ Fourier Transform Infrared spectroelectrochemical measurements have been made to determine if polysulfide intermediates can be detected.

EXPERIMENTAL

Experiments included leaching experiments of chalcopyrite in ferric sulfate solution, electrochemical measurements, and FTIR spectroelectrochemical analysis.

Leaching Experiments

The effect of particulate carbon additions on the initial reaction kinetics for ferric sulfate leaching of $CuFeS_2$ was studied. An experimental technique was developed to obtain contact between chalcopyrite particles and carbon particles. This technique involved intimate mixing of the particles and compression of the mixture to form a pellet which contained $CuFeS_2$/C aggregates. Chalcopyrite and carbon particles were mixed thoroughly and pressed at 20,000 lbs into pellets of 1.3 cm in diameter. The thickness of the pellet depends upon the amount of sample used, but most samples were 0.24 cm thick. The compression and porosity of the pellet depend on the particle size and the proportion of chalcopyrite to carbon.

The chalcopyrite used in these leaching experients was obtained from a Pima flotation concentrate. Monosize chalcopyrite samples were prepared from the concentrate by wet screening and sizing with a Warman Cyclosizer. The chemical analysis of each monosize sample is shown in Table 2.

Table 2.

Chemical Analysis for Prepared Monosize Chalcopyrite Samples

d_{50} size (microns)	Chemical Analysis	
	Cu %	Fe %
4.6	29.95	26.27
12	30.49	26.35
28	30.75	27.25
38	31.58	27.73

Carbons used in this study were obtained from Cabot Carbon Corp. a Fisher Scientific Company.

All acid ferric sulfate leaching experiments were carried out in one-liter cylindrical reactors immersed in thermostatically controlled water baths as described previously (9).

Electrochemical Measurements

Electrochemical measurements were obtained using a typical three-electrode system with a chalcopyrite working electrode for anodic polarization studies (a graphite working electrode was used for cathodic studies), a platinum auxiliary electrode, and a saturated calomel reference electrode. A conventional electrochemical system was used in this study, Princeton Model 173 potentiostat Model 376 logarithmic current converter and Model 175 potential sweep generator. Potentiodynamic polarization experiments were designed to examine the nature of the half-cell reaction. Some of the electrochemical experiments were carried out at elevated temperature. Stirring was achieved by means of a magnetic stirrer.

Three different chalcopyrite electrodes were prepared. Massive chalcopyrite electrodes were prepared from high-quality natural specimens of Transvaal chalcopyrite. Chalcopyrite particulate electrodes and chalcopyrite/carbon aggregate electrodes were prepared from 325x400 mesh particles of the same Transvaal chalcopyrite sample and made into the pellets described above. These pellets were first filled with Polyscience's Spurr low-viscosity embedding resin and cured under vacuum. The Spurr low-viscosity embedding resin has an exceptional penetration property, and thus excellent electrodes were prepared which could be polished with ease.

In all cases, the electrode surface was carefully polished by standard metallographic techniques. The experimental procedure was found to be essential to minimize spurious time-dependent effects due to the presence of superficial oxidation products.

The active surface area of chalcopyrite for particulate or aggregate electrodes was measured by image analysis. The assumption is made for this image analysis that all particles are randomly positioned and oriented in the prepared specimen. Thus, a simple way of characterizing the area of chalcopyrite is by sequentially scanning the projected image of the whole electrode surface. The area percent of chalcopyrite is recorded for each field. The area percent distribution obtained from scanning of the electrodes is shown in Figures 8 and 9. The mean area percentage of $CuFeS_2$ for a typical $CuFeS_2$ particulate electrode is 70.6% while for a typical $CuFeS_2$/C aggregate ($CuFeS_2$:C = 10:1 wt. ratio) is 41%.

Fourier Transform Infrared Spectroscopic Analysis

In addition to the electrochemical measurements, the reaction surface was examined by infrared spectroscopy. A digital Qualimatic Fourier Transform Infrared spectrometer was used. The preliminary study with FTIR spectroelectrochemistry was to analyze the composition and structure of thin reaction product layer formed on chalcopyrite electrode surface. An in-situ measurement was selected because it is a more appropriate method for studying the electrode interface and is able to monitor processes at the electrode interface as the reaction occurs. The details of FTIR spectroelectrochemical measurements are described in the section on Experimental Results.

EXPERIMENTAL RESULTS AND DISCUSSION

The anodic dissolution of chalcopyrite in acidic ferric sulfate solution can be described by the half-cell reaction,

$$CuFeS_2 \rightarrow Cu^{2+} + Fe^{2+} + 2S^o + 4e \qquad (6)$$

forming elemental sulfur. It has been reported that initially a defect chalcopyrite structure forms prior to passivation by the layer of elemental sulfur. Also, some sulfur may be oxidized to sulfate, but the kinetics of sulfate formation in acid ferric sulfate solution are quite slow, and most of the sulfur is present as elemental sulfur. In any case, the formation of a dense and tenacious sulfur layer passivates the reaction and slows the leaching rate to unacceptably low levels. As discussed in the Introduction, the addition of carbon particles reduces passivation to a certain extent and significantly increases the leaching rate, extending the time for surface reaction control.

Initial Kinetics of Ferric Sulfate Leaching of $CuFeS_2$/C Aggregates

During the initial stage of reaction, transport through the reaction-product layer cannot be rate-controlling. The reaction must be controlled by surface chemical reaction and/or transport of reactants. In this study, initial rates were determined by fitting a second-order polynomial regression curve to the rate data and taking the limit of the derivative ($d\alpha/dt$) as time t approaches zero. This approach provides only an estimate of the initial rates. The initial rate of $CuFeS_2$/C aggregate is three times faster than that of $CuFeS_2$ in the absence of carbon (Figure 10). These initial rate data will be compared to electrode reaction rates in the next section as an indication of their significance.

The temperature effect on the initial leaching kinetics of 38-μm chalcopyrite particles with the addition of carbon was studied. Initial rate data from experimental results were plotted in the form of an Arrhenius plot as shown in Figure 11, and an activation energy of 38.1 kJ/mole (9.1 kcal/mole) was obtained. This activation energy is close to the activation energy for the initial kinetics of chalcopyrite leaching without carbon addition, which was found to be 33.5-50 kJ/mole (8-12 kcal/mole) (1,17). Figure 12 shows the effect of ferric sulfate concentration on the initial kinetics. From the plot of initial reaction rate versus ferric ion concentration, the order of reaction with respect to ferric concentration seems to approach one-half, typical of many surface reaction-controlled electrochemical reactions.

The chalcopyrite particle size effect has been studied, and the beneficial effect of carbon addition seems to be more pronounced for coarse chalcopyrite particles (5). The significance of the breakage of coarse chalcopyrite particles during compaction of the aggregate has been observed, but such breakage is not significant for the smaller chalcopyrite particles. Nevertheless, a linear relationship between the initial reaction rate and inverse particle diameter (after compression) is obtained as shown in Figure 13. Thus, this supports the notion that a surface reaction may be the initial rate-controlling step.

The kinetic aspects of ferric sulfate leaching of $CuFeS_2$/C aggregates are complicated. More than one rate process may be involved (9). From the initial kinetic studies, the apparent initial rate of reaction approaches one-half order with respect to ferric concentration, which in conjunction with the particle size dependence and an activation energy of 38.1 kJ/mole (9.1 kcal/mole) suggests that the initial reaction rate is controlled by an electrochemical surface reaction similar to that which occurs in the absence of carbon particles. Further, in the presence of carbon particles, this surface reaction limitation has greater kinetic significance than in the absence of carbon particles. In the absence of carbon particles, the surface reaction resistance can be ignored and the reaction rate explained

satisfactorily by parabolic kinetics alone. On the other hand, in the presence of carbon particles, the rate is under mixed control and the surface reaction must be considered to adequately describe the reaction kinetics.

Electrochemical Measurements

Electrochemical measurements provide additional data for the analysis of initial reaction kinetics. The initial leaching rate with carbon was found to be three times faster than the initial rate without carbon addition. These results may be indicative of a change in the mechanism of the controlling half-cell reaction or may relate to other aspects of the leaching reaction. The electrochemical data will be presented to demonstrate the effect of carbon on the initial kinetics.

The polarization curves for the anodic half-cell reaction of massive chalcopyrite, particulate chalcopyrite, and $CuFeS_2$/C aggregate electrodes are compared in Figure 14. The shape of the polarization curves for the massive chalcopyrite and particulate chalcopyrite electrode are similar; however, the passivation region of the massive chalcopyrite electrode is more significant. The $CuFeS_2$/C aggregate electrode did not exhibit this passivation effect during anodic polarization and gave an anodic current significantly greater than the corresponding current for chalcopyrite without carbon in the passive region. This observation may help to explain the observed increase of the initial leaching rate.

A convenient way to think about electrochemical reaction kinetics is to plot the current/potential curves for the respective half-cells involved in the leaching reaction. Electrochemical processes are unique in that the solid may assume a uniform potential throughout, provided ohmic resistance is negligible. The potential may directly affect the kinetics of the reaction if slow discharge is involved and may also serve to stabilize intermediate solid phases. If one or more electrode reactions occur simultaneously, a mixed potential may exist. The current/potential curves for the massive chalcopyite electrode and the $CuFeS_2$/C aggregate electrode are presented in Figures 15 and 16 both in the presence and absence of ferric sulfate. The corrosion cell which results in the anodic oxidation of chalcopyrite and the cathodic reduction of ferric ion is as follows:

$$CuFeS_2 \rightarrow Cu^{2+} + Fe^{2+} + 2S^0 + 4e \qquad (6)$$

or the intermediate anodic reaction,

$$CuFeS_2 \rightarrow Cu_{1-x}Fe_{1-y}S_{2-z} + xCu^{2+} + yFe^{2+} + zS^0 + 2ze^- \qquad (2)$$

and

$$Fe^{3+} + e \rightarrow Fe^{2+} \qquad (7)$$

The polarization curves for the cathodic half-cell reactions are calculated and plotted as dashed lines in these figures. Also in the case of the $CuFeS_2$/C electrode (Figure 16), the cathodic polarization curve for reduction of ferric ion was determined experimentally using a graphite electrode and is seen to be in good agreement with the calculated curve.

For chalcopyrite dissolution, the mixed potential (or the potential of zero current) is a corrosion potential and the corrosion current represents the rate of chalcopyrite dissolution. Three electrochemical processes can contribute to the currents during the corrosion of chalcopyrite in ferric sulfate solution. These are the oxidation of chalcopyrite, the reduction of ferric ion on the corroding $CuFeS_2$ surface, and the oxidation of ferrous ion on the corroding chalcopyrite surface. Because of the passive product film formed on the chalcopyrite surface, the anodic currents are remarkably insensitive to changes of potential between 0.3-0.6 v (vs. SCE) as shown in Figure 14. The corrosion current is limited under these circumstances due to the passivating film. This behavior should be contrasted to the behavior of the $CuFeS_2$/C electrode as shown in Figure 16 in which there is no evidence of passivation. In this regard, it should be noted that the scale of current density in Figure 16 is five times larger than that in Figure 15.

When chalcopyrite is in electrical contact with carbon particles, galvanic interaction may occur which can cause an enhanced corrosion of the electrochemically coupled reactions. Chalcopyrite with the lower rest potential will react anodically, whereas graphite or carbon which possesses a higher rest potential will react cathodically. The galvanic coupling between graphite and chalcopyrite within the leaching environment will establish a mixed potential or corrosion potential as shown in Figure 16. Under this condition, graphite is an inert electrode, the ferric oxidant is discharged cathodically at the graphite surface, and the galvanic leaching mechanism can be depicted in Figure 17 showing the electron transfer from the anodic chalcopyrite particle, resulting in the discharge of oxidant species at the graphite surface.

Other electrochemical results were obtained from chronoamperometry experiments. At constant potential, a plot of current versus time represents the rate of oxidation. The cumulative quantities of charge calculated according to the measured current and the corresponding time are plotted as a function of time in Figure 18 for different types of chalcopyrite electrodes. Both the particulate chalcopyrite electrode and $CuFeS_2$/C aggregate electrode show the current decay with time but are not as significant as that observed for the massive chalcopyrite (12). At 82°C, 500 mv, copper is produced at a rate of

1.58×10^{-10} moles/cm^2-sec for the particulate chalcopyrite electrode after 60 minutes. Under the same conditions, the $CuFeS_2$/C aggregate electrode gave a dissolution rate of 9.2×10^{-10} moles/cm^2-sec. These results and the dissolution rate calculated from the corrosion currents at the mixed potential for the $CuFeS_2$/C aggregate electrode indicate that the anodic dissolution rate is five times faster than for chalcopyrite electrodes in the absence of carbon. Fair agreement is achieved between the rate for potentiostatic electrochemical oxidation and the leaching reaction rate. As mentioned previously the initial leaching rate for $CuFeS_2$/C aggregates is three times faster than the initial rate for chalcopyrite particles without carbon.

The anodic polarization curves for the $CuFeS_2$/C aggregate electrode in 1 M H_2SO_4 at different temperatures were traced with the potentiostat as shown in Figure 19. The anodic current increased significantly as temperature increased. At the mixed potential the corresponding currents for different temperatures were determined and plotted against the inverse absolute temperature to determine the activation energy. An activation energy of 46 kJ/mole (11 kcal/mole) is consistent with that determined from initial leaching rate experiments.

Some of the difference between the leaching data and the electrochemical measurements is explained because the estimate of the initial rate from leaching data is limited due to the experimental technique. In the case of the estimate of the initial rate from leaching data, the reaction has proceeded to a greater extent and the passivation is more significant than that observed from electrochemical data. However, it seems in both cases that the mechanism is the same because of the similar activation energies and reaction orders.

FTIR Spectroelectrochemistry

The electrochemical methods for studying dissolution kinetics include galvanostatic and potentiostatic measurements which have been supplemented in some cases by potentiodynamic studies, a-c impedence investigations, and coulometry. These methods have been useful in characterizing the anodic behavior of electrodes, but the electrochemical techniques do not provided unambiguous information about the chemical composition and structure of anodically produced surface films. Nonelectrochemical techniques used thus far have also been of limited value. Electron diffraction investigations require that the specimen be removed from its environment, and reasonable objections to the interpretation of the results can be raised because of possible changes in composition of the specimen surface, such as dehydration. Although ellipsometry is a highly surface-sensitive technique and is applicable to in-situ studies, the technique only measures film thickness. In-situ FTIR spectroscopy offers the possibility of obtaining direct compositional and structural information about thin anodic

films. Research has been initiated to evaluate the emission IR spectra for in-situ chemical characteristics of reaction intermediates at a chalcopyrite electrode under anodic bias.

Chalcopyrite itself contains infrared active bonds which should appear below 400 cm^{-1} (18). Reaction products such as polysulfide films or elemental sulfur would be expected to contain infrared active S-S bonds, having vibrational frequencies between 460-480 cm^{-1} (29-21) and 663 cm^{-1} (see Figure 21). In this regard, FTIR measurements may provide further information about the reaction product intermediate.

The spectroelectrochemical experiment is a reflectance experiment, in which infrared radiation is reflected off the surface of a polished electrode sitting in an electrochemical cell (see Figure 20). and the reflected light is detected.

The resulting single-beam spectrum contains absorption bands due to absorbing species, in solution and on the electrode surface, but also contains the wavenumber dependence of instrumental energy throughput, detector sensitivity, and electronic response. To remove the latter contributions, it is usual to present difference spectra, which show only changes in absorption caused by a change in some variable, such as electrode potential.

Spectroelectrochemical experiments were carried out as follows: A polished chalcopyrite electrode was inserted into a cell containing an aqueous solution of 0.1 M $HClO_4$. The solution was degassed by bubbling helium through it for about 15 minutes. The working electrode was then pushed against an infrared-transparent ZnSe window. This left a layer of solution about 1-10 μm thick between electrode and window, minimizing absorption of the radiation by the water. In order to detect the very small signals due to changes at the electrode surface, an FTIR spectrometer (Digilab Qualimatic) was used which allows rapid collection of many spectra. These spectra can be averaged to increase the signal/noise ratio. Typically, one set of spectra was collected over a 10-minute period with the electrode at open circuit. A second set was then collected with the electrode at a controlled potential where a reaction intermediate was expected to form. The average of the second set was divided by the average of the first set to give what is essentially a difference spectrum. Peaks pointing up correspond to species present at open circuit which are destroyed at the controlled potential, and peaks pointing down correspond to peaks not present at open circuit but which are formed at the controlled potential. The spectra of the electrode surface can therefore be monitored both as a function of potential and of time at constant potential.

Spectra were obtained over a potential range of 450 mV to 1200 mV (SCE), and at times varying from a few minutes to several hours. An example is presented in Figure 21. Some peaks are found in the range of the S-S bonding frequency but did not change in a very systematic

manner with potential or time. Nevertheless, these results are preliminary and further research is in progress.

CONCLUSIONS

1. The very slow dissolution rate of the ferric sulfate leaching of chalcopyrite can be improved by the addition of carbon to form aggregates. In the presence of carbon, the leaching rate increases substantially and initial rate control by an electrochemical surface reaction becomes evident.

2. The initial rate of the ferric sulfate leaching of $CuFeS_2$/C aggregates was found to be one-half order with respect to ferric concentration, and inversely proportional to the initial particle diameter, with an apparent activation energy of 38.1 kJ/mole (9.1 kcal/mole). These results suggest that the initial reaction rate is controlled by surface reaction.

3. Electrode measurements both in the presence and absence of carbon support electrochemical analysis of the initial reaction kinetics. The galvanic coupling between carbon and chalcopyrite eliminates the ohmic resistance of passive reaction product films and as a result higher current densities are realized. The rate of potentiostatic electrochemical oxidation for the $CuFeS_2$/C aggregate electrode is five times faster than the rate for the particulate $CuFeS_2$ electrode.

4. In-situ Fourier Transform Infrared Spectroscopic measurements have been made to detect the nature of the initial surface reaction product at the chalcopyrite surface. The preliminary results have not been conclusive but have demonstrated the potential utility of in-situ FTIR spectroscopy for sulfide electrodes in the further study of leaching reaction mechanisms.

ACKNOWLEDGEMENTS

The research activity has been supported by funds from the Mineral and Primary Materials Processing Program, National Science Foundation Grant No. 81-07763. Our grateful acknowledgement is made to Prof. I. M. Ritchie, Dr. R. Woods, and Prof. M. E. Wadsworth for their interest and helpful discussions.

REFERENCES

1. P. B. Munoz, J. D. Miller, and M. E. Wadsworth, "Reaction Mechanism for the Acid Ferric Sulfate Leaching of Chalcopyrite," Met. Trans. B, vol. 10B, 149-158 (1979).

2. D. E. Lowe, "The Kinetics of the Dissolution Reaction of Copper and Copper-Iron Sulfide Minerals Using Ferric Sulfate Solutions," Ph.D. Thesis, University of Arizona, Tucson, Arizona (1970).

3. L. W. Beckstead et al., "Acid Ferric Sulfate Leaching of Attritor-Ground Chalcopyrite Concentrates," Extractive Metallurgy of Copper, vol. 2, AIME, 611-632 (1976).

4. J. E. Dutrizac, "The Dissolution of Chalcoyrite in Ferric Sulfate and Ferric Chloride Media," Met. Trans. 12B, 371-378 (1981).

5. R. Y. Wan, J. D. Miller, H. J. Wei, and G. Simkovich, "The Significance of Carbon Properties in the Enhanced Ferric Sulfate Leaching of $CuFeS_2$/C Aggregates," submitted for publication.

6. Jose Raul Fernandez, "Continuous Leaching of Attritor-Ground Chalcopyrite in Acid Ferric Sulfate Solution," Ph.D. Thesis, University of Utah, Salt Lake City, Utah, 1978.

7. C. Wagner, "The Electrical Conductivity of Semi-Conductors Involving Inclusions of Another Phase," J. Phys. Chem. Solids, 3B, 1051 (1972).

8. G. Simkovich et al., "The Electrical Conductivity Behavior of Monarch 1100 Carbon Plus Sulfur from 308 to 368 K," in preparation for publication.

9. R. Y. Wan, J. D. Miller, and G. Simkovich, "Enhanced Ferric Sulfate Leaching of Copper from $CuFeS_2$/C Particulate Aggregates," Proceedings of Mintek 50 -- An International Conference on Recent Advances in Mineral Science and Technology, South Africa, March 1984.

10. T. Biegler and D. A. Swift, "Anodic Electrochemistry of Chalcopyrite," Journal of Applied Electorchemistry, 9, 545-554 (1979).

11. D. L. Jones, Ph.D. Thesis, Department of Metallurgy, The University of British Columbia, Vancouver, B.C., 1974.

12. G. W. Warren, "Electrochemical Oxidation of Chalcopyrite," Ph.D Thesis, University of Utah, Salt Lake City, Utah, December, 1978.

13. G. W. Warren, M. E. Wadsworth, and J. M. El-Raghy, "Passive and Transpassive Anodic Behavior of Chalcopyrite in Acid Solutions," Met. Trans. B, vol. 13B, 571-579 (1982).

14. P. J. Parker, R. L. Paul, and G. P. Power, "Electrochemical Aspects of Leaching Copper from Chalcopyrite in Ferric and Cupric Salt Solutions," Aust. J. Chem., 34, 13-34 (1981).

15. E. Hillrichs, H. Geulich, and R. Bertram, "Investigations of the Electrochemical Dissoluton of Sulfide Ores in Sulfuric Acid Solutions," Hydrometallurgy Research, Development and Plant Practices, edited by K. Osseo-Asare and J. D. Miller, 277, 1983.

16. A. J. Parker, R. L. Paul, and G. P. Power, "Electrochemistry of the Oxidative Leaching of Copper from Chalcopyrite," J. Electroanalytical Chemistry, 118, 305-316 (1981).

17. J. P. Baur, H. L. Gibbs, and M. E. Wadsworth, "Initial Stage Sulfuric Acid Leaching Kientics of Chalcopyrite Using Radiochemical Techniques," U.S.B.M. RI 7823 (1974).

18. A. Miller, A. MacKinnon, and D. Weaire, "The Chalcopyrite and Related Semiconducting Compounds," Solid State Physics, vol. 36, p. 150 (1981).

19. A. W. Herlinger et al., Inorganic Chemistry, vol. 12, 2661 (1969).

20. K. Nakamoto, Infrared and Raman Spectra of Inorganic and Coordination Compounds, 1978, John Wiley and Sons, Inc.

21. L. J. Bellamy, The Infrared Spectra of Complex Molecules, 1960.

Table 1. The Conductivity of C/S Composites for Different Types of Carbon and the Leaching Response of $CuFeS_2$/C Aggregates.

Carbon Type	σ_1^* 5% C/S Composite $(ohm\text{-}cm)^{-1}$	σ_2^* 15.9% C/S Composite $(ohm\text{-}cm)^{-1}$	Fraction of Cu Reacted from $CuFeS_2$/C Aggregates after 10 hrs
Pearl 2000	2.6×10^{-2}	2.2×10^{-1}	0.560
Monarch 800	1.05×10^{-3}	-	0.524
Monarch 1100	9.0×10^{-4}	-	0.488
Lonza KS-2.5	5.4×10^{-4}	1.6×10^{-1}	0.322
Spheron 6	2.2×10^{-4}	-	0.314
Fisher 38	-	6.2×10^{-2}	0.316
Cerac Pure	-	9.1×10^{-2}	0.281
Calgon Activated Carbon	-	2.4×10^{-3}	0.209
		Conductivity $(ohm\text{-}cm)^{-1}$	
Chalcopyrite (no carbon)		$\sim 10^{+1}$	0.067
Pure Sulfur		$\sim 10^{-13}$	

*σ_1 and σ_2 are measured at 5 vol. % and 15.92 vol. % carbon, respectively, in pure sulfur at 90°C.

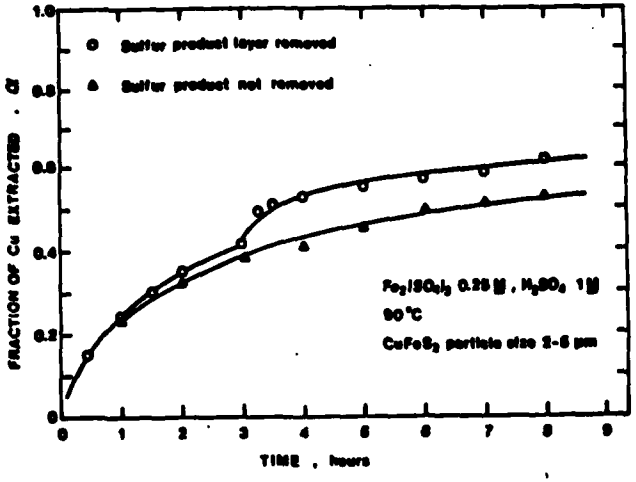

Figure 1. The fraction of Cu extracted from chalcopyrite particles as the leaching reaction is interrupted and the elemental sulfur product layer is removed by distillation under N_2 atmosphere after 3 hrs' leaching.

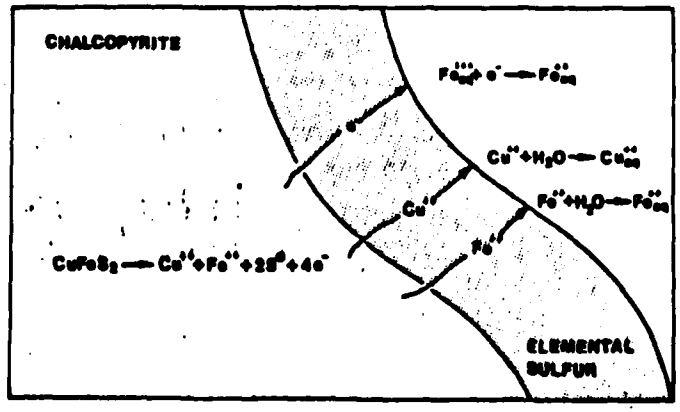

Figure 2. Schematic representation of the transport process in the ferric sulfate leach of chalcopyrite.

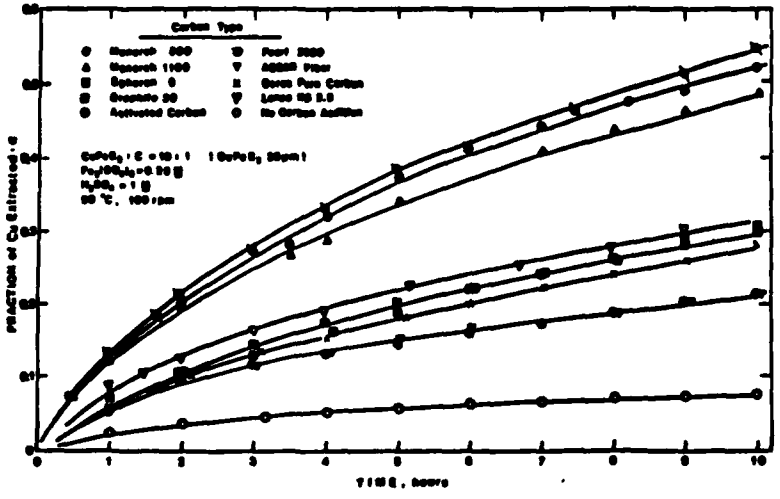

Figure 3. Fraction of Cu extracted from $CuFeS_2$/C aggregates prepared with different carbon types.

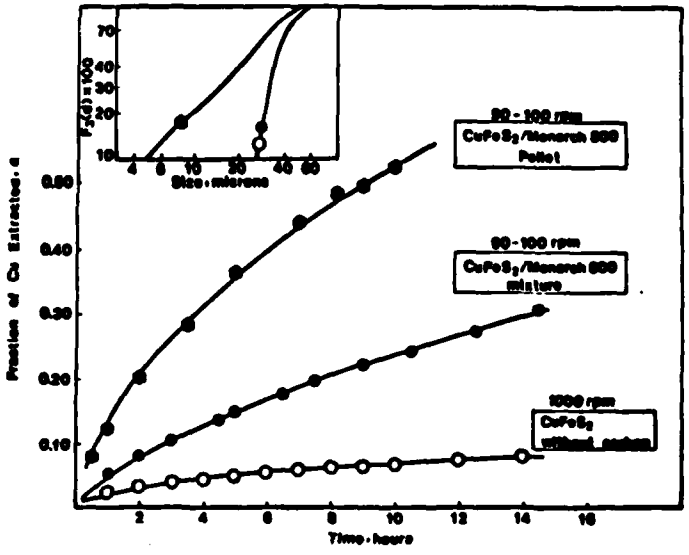

Figure 4. Fraction of Cu extracted from $CuFeS_2$/C pellet; $CuFeS_2$/C mixture and $CuFeS_2$ particles without carbon addition. $CuFeS_2$ mixed with Monarch 800 carbon ($CuFeS_2$:C = 25:1), 90°C, $Fe_2(SO_4)_3$ 0.25 M, H_2SO_4 1 M.

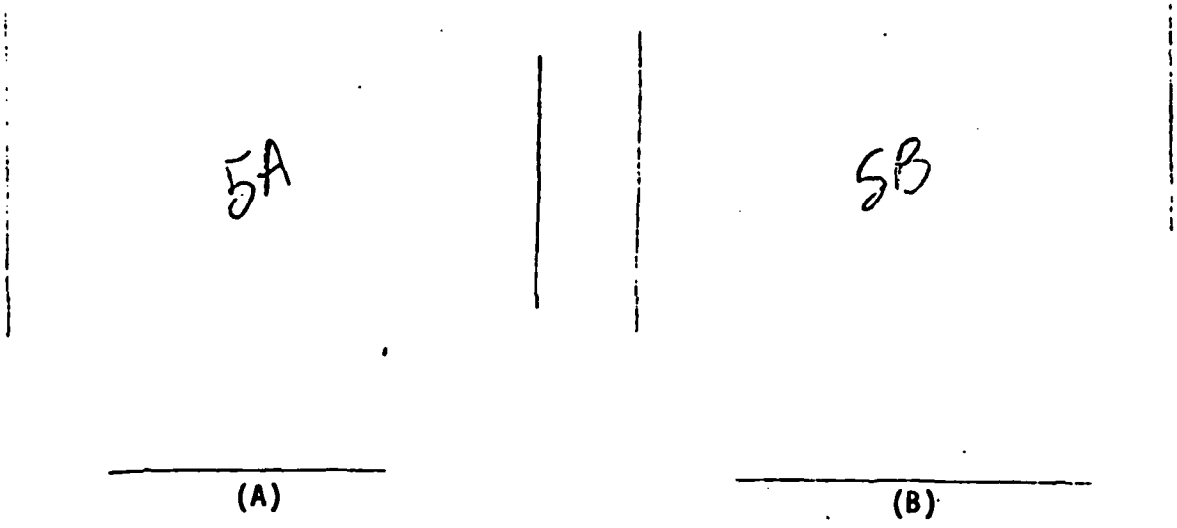

(A) (B)

Figure 5. SEM photomicrograph of partially leached chalcopyrite/carbon aggregate by ferric sulfate solution; (A) d_o = 38 μm, α = 0.27; (B) d_o = 38 μm; α = 0.58

(A) (B)

Figure 6. SEM photomicrograph of partially leached chalcopyrite particle by ferric sulfate solution; (A) d_o = 38 μm; α = 0.17; (B) d_o = 12 μm, α = 0.20.

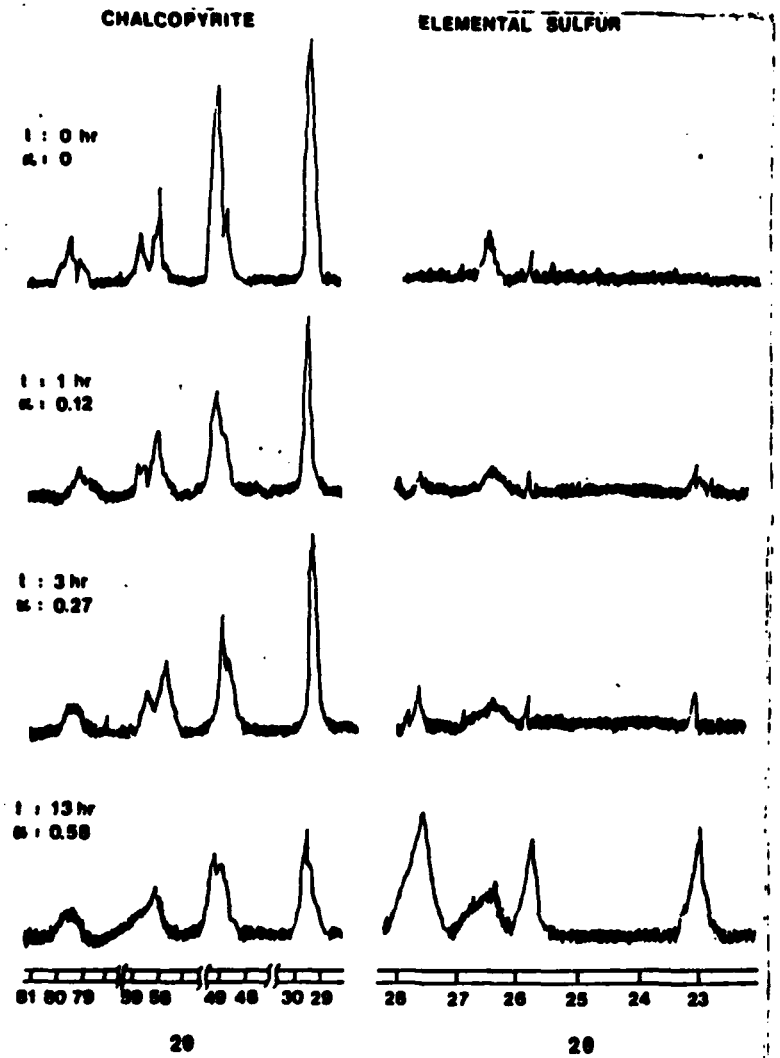

Figure 7 X-ray diffraction pattern of original chalcopyrite sample and leaching residues at different extents reaction α = 0.12, 0.27, 0.58.

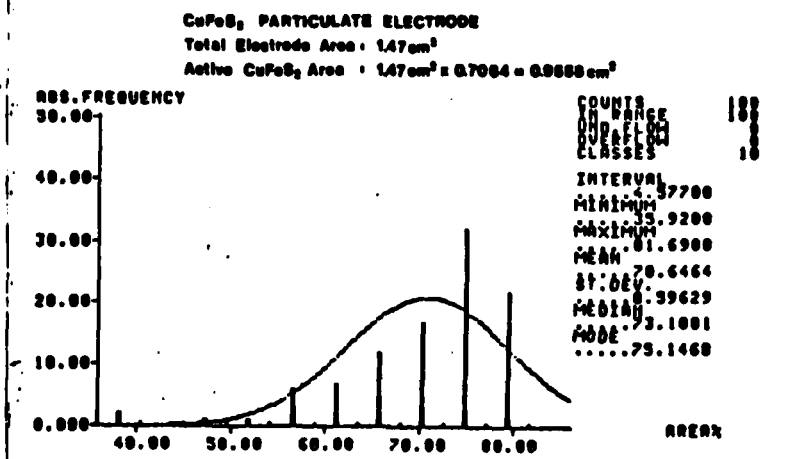

Figure 8 Area percent distribution of chalcopyrite obtained from image analysis for $CuFeS_2$ particle electrode.

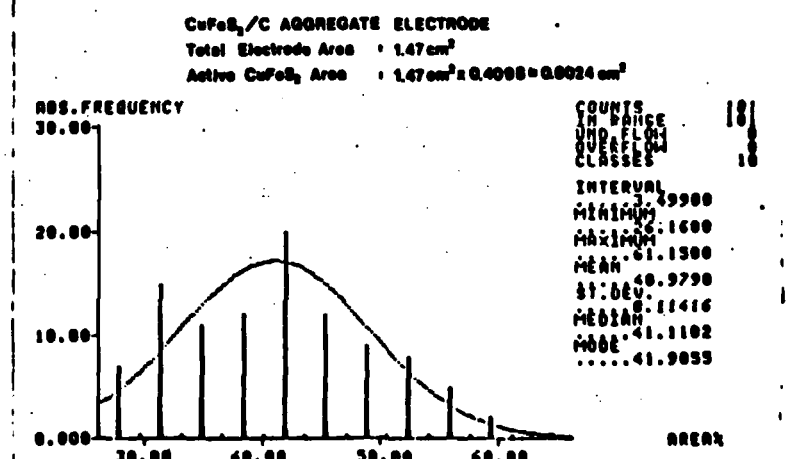

Figure 9 Area percent distribution of chalcopyrite obtained from image analysis for $CuFeS_2$/C aggregate electrode.

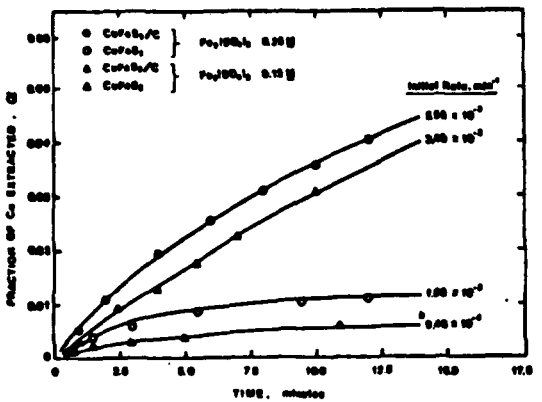

Figure 10 Fraction of Cu Extracted for the Initial Leaching of $CuFeS_2$/C aggregates and chalcopyrite particles without carbon addition at 90°C. $CuFeS_2$: monarch 800 = 25 : 1 [a]Data from Ref (1).

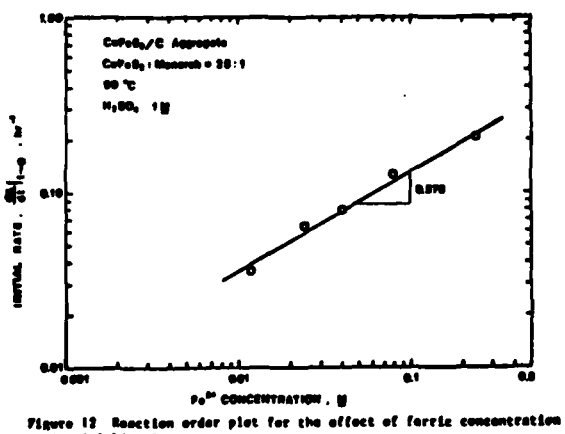

Figure 12 Reaction order plot for the effect of ferric concentration on initial kinetics.

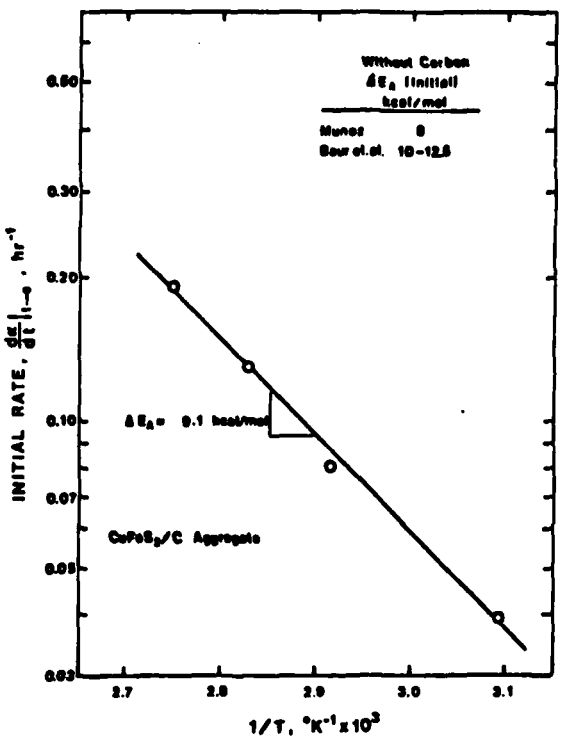

Figure 11 Arrhenius plot based on initial reaction rate data.

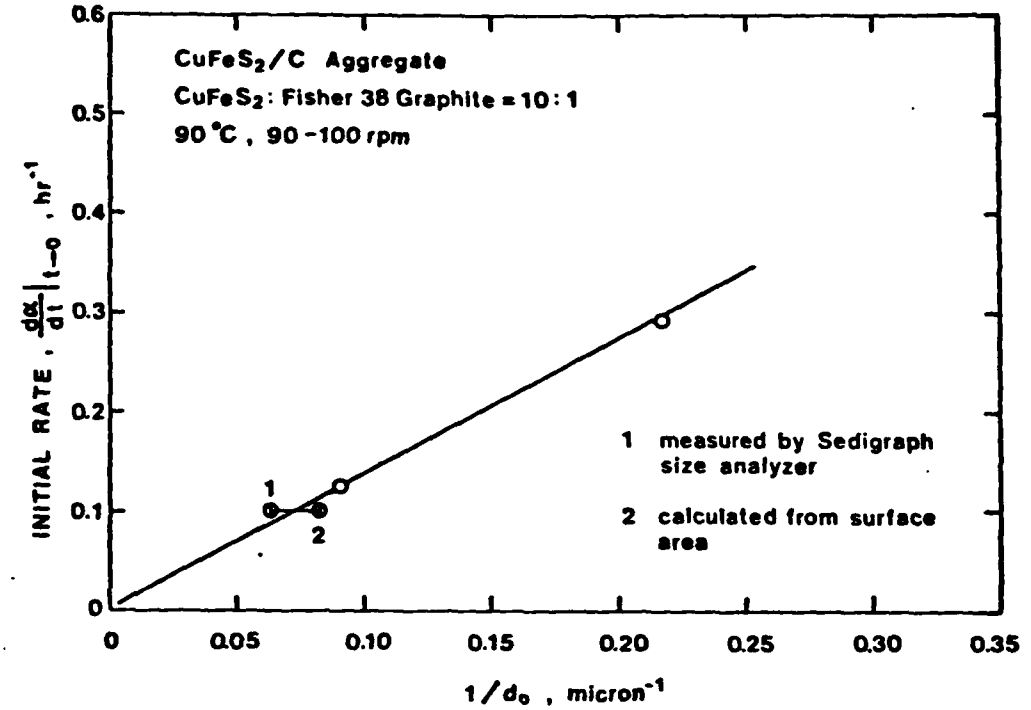

Figure 13 Initial rate as a function of inverse initial particle diameter.

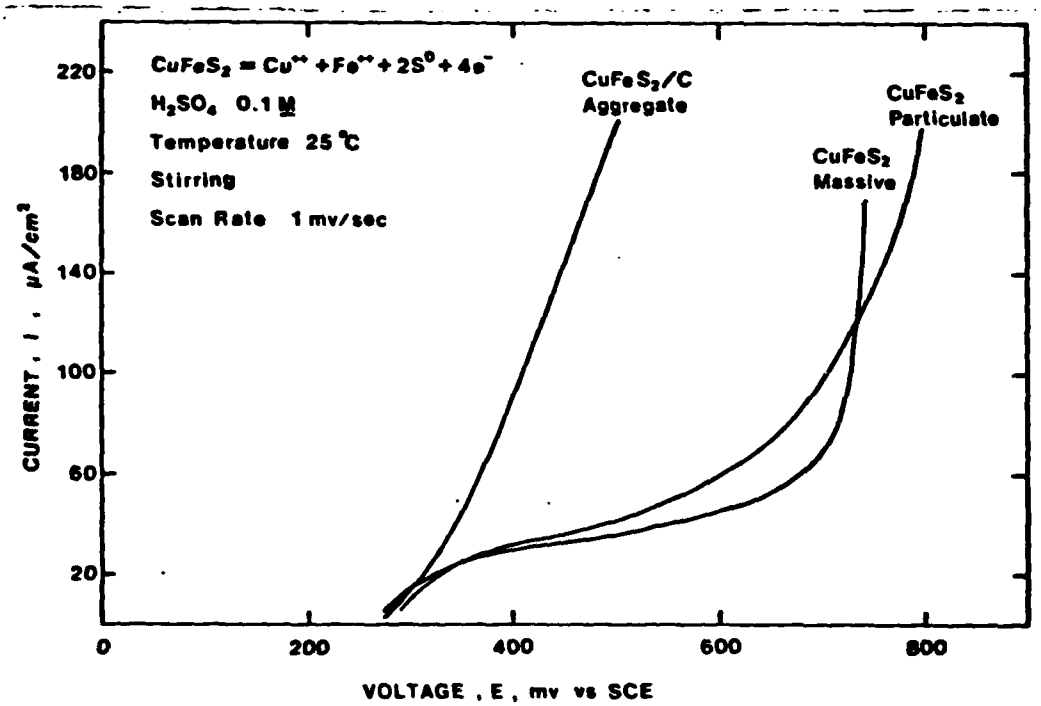

Figure 14 Polarization curves for the anodic reaction of massive chalcopyrite, particulate chalcopyrite and $CuFeS_2$/C aggregate electrodes.

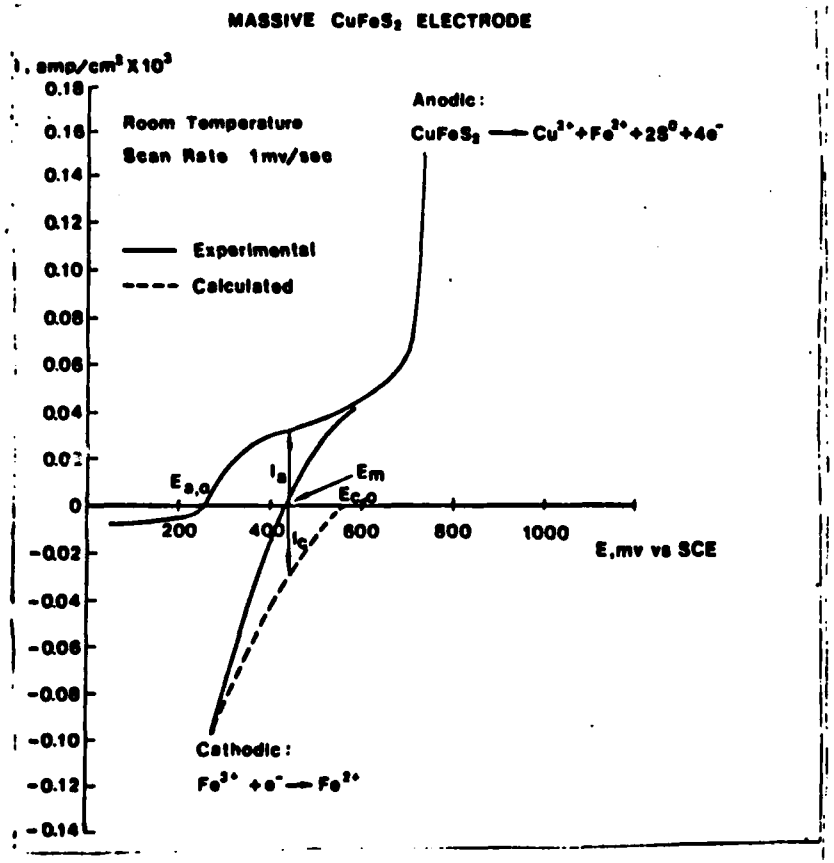

Figure 15 Current-potential behavior for a massive chalcopyrite electrode, 25°C.
anodic polarization curve, H_2SO_4 0.1 M.
corrosion curve: $Fe_2(SO_4)_3$ 0.1 M, $FeSO_4$ 0.01 M, H_2SO_4 0.1 M.

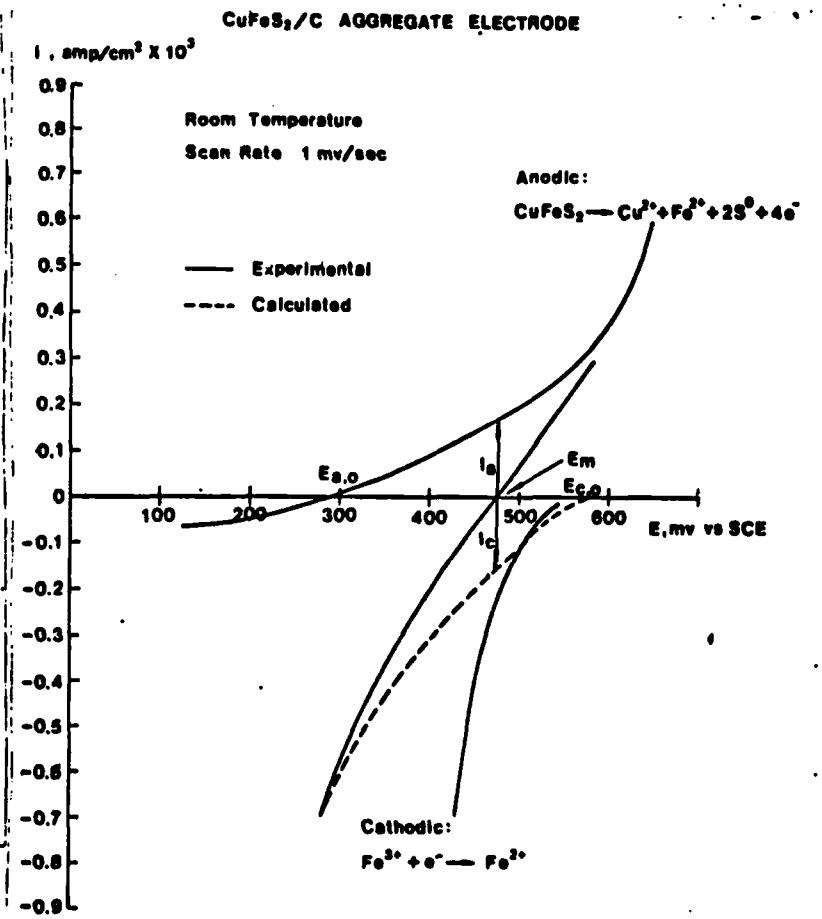

Figure 16 Current - potential Behavior for a CuFeS2/C aggregate electrode, 25°C
anodic polarization curve: H_2SO_4 0.1 M.
corrosion curve: $Fe_2(SO_4)_3$ 0.1 M, $FeSO_4$ 0.01 M, H_2SO_4 0.1 M
cathodic polarization curve: $Fe_2(SO_4)_3$ 0.1 M, $FeSO_4$ 0.01 M, H_2SO_4 0.1 M.

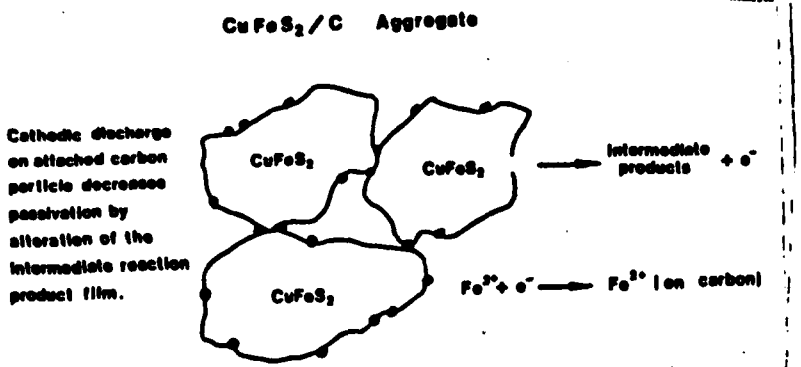

Figure 17 Schematic representation of the initial ferric sulfate leaching of $CuFeS_2$/C aggregates.

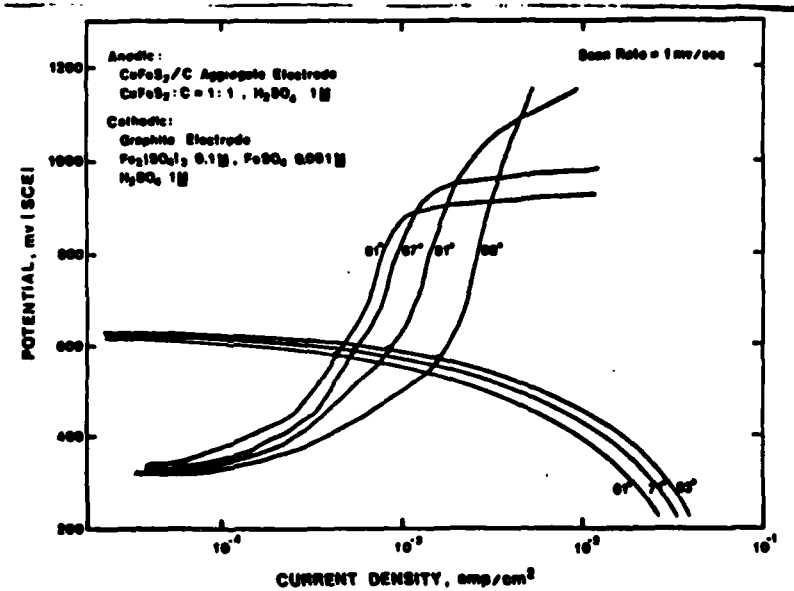

Figure 19 Temperature effect on anodic polarization curves for $CuFeS_2$ aggregate electrode and cathodic polarization curves using a graphite electrode.

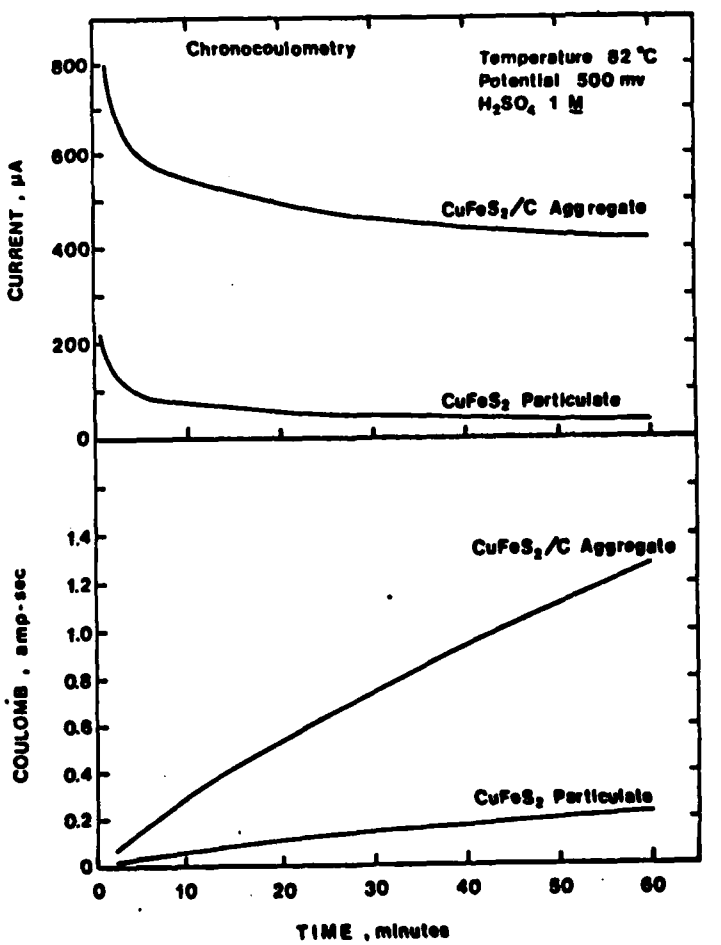

Figure 18 Plots of current and charge versus time for particulate $CuFeS_2$ electrode and $CuFeS_2$/C aggregate electrode at 80°C, 500 mv in $1M\ H_2SO_4$.

SCHEMATIC DIAGRAM OF ELECTROCHEMICAL INFRARED CELL

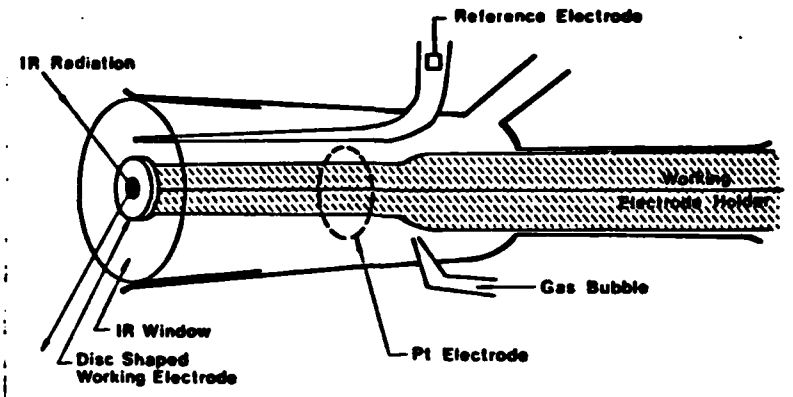

Figure 20 Schematic Diagram of an Electrochemical In-Situ FTIR Cell.

FTIR IN-SITU SPECTRA FOR $CuFeS_2$

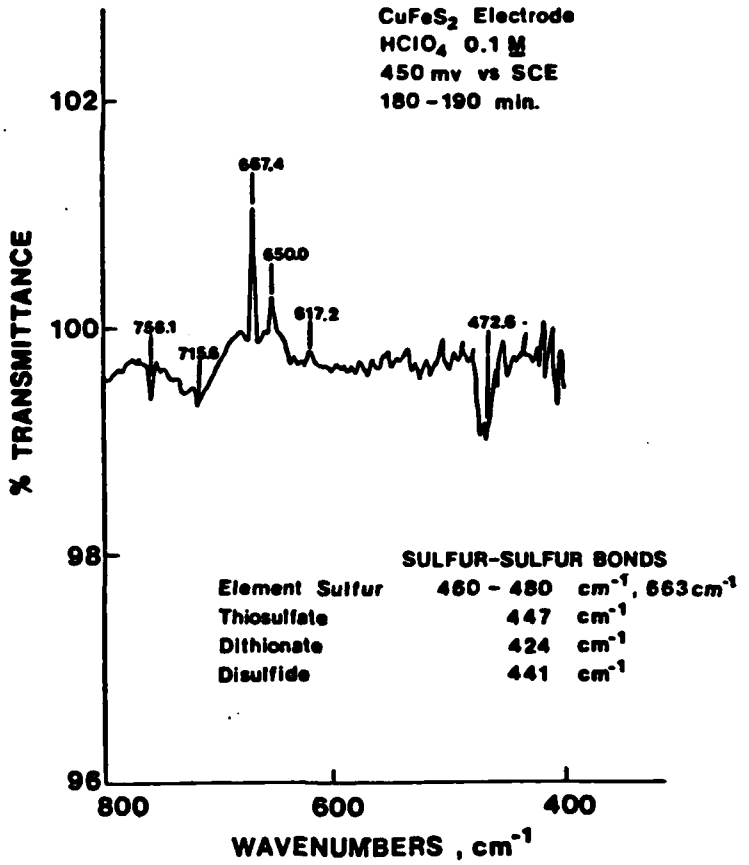

Figure 21 FTIR In-Situ spectra for $CuFeS_2$ at 450 mv (vs SCE).

END

FILMED

1-85

DTIC